



Anal. Bioanal. Chem. Res., Vol. 11, No. 3, 291-298, July 2024.

On-Chip Preconcentration and Determination of Magnetite Nanoparticles in Water Based on Paired Emitter-Detector Diode Photometry

Yaser Younesi Vakil and Mazaher Ahmadi*

Department of Analytical Chemistry, Faculty of Chemistry and Petroleum Sciences, Bu-Ali Sina University, Hamedan, Iran

(Received 26 February 2024, Accepted 27 March 2024)

Iron oxide nanoparticles have been widely used in various fields of study. Due to the increasing use of these nanoparticles, it is important to develop sensitive methods for measuring these nanoparticles in real samples. In this research, a method was developed to measure magnetite nanoparticles using microfluidics science and paired emitter-detector diode-based photometry. The basis work of the designed system is based on the magnetic preconcentration of nanoparticles inside the microchip, dissolution by acid, and creation of a signal through the formation of an iron-thiocyanate complex. The validation results of the method showed that the linear range of the method is from 1.0 to 6.0 ppm with appropriate accuracy (recovery percentages: 104.0% and 95.6%) and precision (coefficient of variation: 0.17% and 0.15%), which is satisfactory for measuring trace amounts of magnetic nanoparticles. The limits of detection and quantification were obtained as 0.3 and 0.9 ppm, respectively. Compared to previously reported methods, the developed method provides higher sensitivity and simpler instrumentation of lower analysis cost by the use of a microfluidic chip for magnetic preconcentration of magnetic nanoparticles, washing, dissolution, and photometric determination.

Keywords: Microfluidics, Iron oxide magnetic nanoparticles, Preconcentration, Determination, Paired emitter-detector diode photometry

INTRODUCTION

Magnetic nanoparticles have recently emerged in many industrial applications related to biomedical, environmental, and clinical disciplines. Such a variety of inapplicability of magnetic nanoparticles was accompanied by new technical challenges related to their fate, toxicity, long-term behavior, disposal and/or recycling, and stability. Various structures of magnetic nanoparticles interact differently with biological life at all levels based on their physical and chemical structures. The toxicity of magnetic nanoparticles can have severe detrimental effects that may even lead to serious damage and collapse of (human) organic systems. Upon fully utilizing magnetic nanoparticles, many techniques have been developed or customized to either dispose of or recycle them. Magnetic nanoparticles will play a major role in modern

diagnostic and therapeutic medicine (*e.g.*, theranostics). Careful and well-controlled use of magnetic nanoparticles will certainly improve the overall quality of life and decrease mortality in several diseases, including different types of cancers, and cardiovascular and developmental disorders [1]. Therefore, there is a need for sensitive methods for the quantification of magnetic nanoparticles.

Quantitative detection methods of magnetic iron oxide nanoparticles are limited to nuclear magnetic resonance (NMR), spectrophotometry, and inductively coupled plasma elemental analysis. NMR can be used to investigate the properties of magnetic nanoparticles, including surface chemistry and interactions with other molecules. Minin *et al.* utilized solid-phase NMR-relaxometry for the determination of 1,2-distearoyl-sn-glycero-3-phosphoethanolamine-poly(ethylene glycol) (DSPE-PEG) modified iron nanoparticles coated with a carbon shell (Fe@C-PEG). The nitrocellulose membranes were chosen as a solid phase [2].

*Corresponding author. E-mail: m.ahmadi@basu.ac.ir

The measurements of the T2 relaxation time for water protons after fixing magnetic nanoparticles from aqueous suspensions in porous membranes allowed the particle concentration to be determined in the range from 0.1 ng mm⁻² to 12 ng mm⁻² of the membrane. The current development of the standard ISO/DTS 19807-1 for the magnetic nanosuspensions highlighted the utmost relevance of the determination of the iron content by inductively coupled plasma-optical emission spectroscopy (ICP-OES) and inductively coupled plasma mass spectrometry (ICP-MS). Costo *et al.* utilized ICP-OES and a spectrophotometry method for the determination of iron content in iron oxide nanoparticles [3]. The spectrophotometry method includes dissolution of the nanoparticles in concentrated hydrochloric acid and reducing Fe³⁺ to Fe²⁺ ions using hydroxylamine hydrochloride before their complexation with 1,10-phenanthroline and consequent spectrophotometric determination at 510 nm wavelength. The linear concentration ranges were 1-20 ppm Fe for ICP-OES and 2.5-20 ppm Fe for spectrophotometry. Recently, Fernández-Afonso *et al.* developed a smartphone-based colorimetric method to quantify the iron concentration of suspensions of magnetic nanoparticles [4]. A series of dilutions of a wide library of magnetic nanoparticles, composed of iron oxide materials in the range between 3 and 43 nm, with two different shapes and four different coatings was prepared. A linear relationship between the G/R ratio from iron oxide nanoparticle suspensions (cubic polyacrylic acid-coated nanoparticles) and their iron concentration has been found in the range between ≈ 0.1 -0.2 and ≈ 1 -3 mg Fe ml⁻¹, depending on the particle size.

Visible light-emitting diodes (LEDs) were developed in 1962 [5] containing p-n junctions emitting a narrow band of light wavelengths [6]. LEDs have found a wide application for the miniaturization of optical sensors due to their low cost, small size, robustness, and high efficiency. They are also used as light detectors since upon light incident, a potential difference is generated across the p-n junction [7]. Therefore, LEDs can be used as both the light source and the detector in paired emitter-detector diodes (PEDD) optical sensors [8,9]. PEDD-based photometers provide low fabrication cost, low power consumption, ease of miniaturization, and a high signal-noise ratio response in a large wavelength range [6]. Furthermore, their output is a

direct pulse-duration-modulated signal, eliminating the need for a costly analog-to-digital converter [10]. These advantages have led to the utilization of PEDD-based optical sensors in various miniaturized photometers as well as a flow-through optical sensor for chromatography and flow analysis [11-13].

This work reports on the development of a method for the quantitative detection of magnetite nanoparticles in water samples by integrating microfluidics magnetic preconcentration to PEDD detection technique. Magnetic sensors can detect and characterize magnetic nanoparticles in microfluidic chips. Magnetic field sensors and detectors are widely used in various applications. Various types of magnetic sensors, including superconducting quantum interference device, magnetoelectric sensors, anisotropic/giant/tunneling magnetoresistive sensors, magneto relaxometry-based sensors, optically pumped sensors, Hall effect sensors, and so on are available [14]. However, the aim of these sensors is not to determine magnetic nanoparticles alone. In fact, the magnetic nanoparticles are part of these sensors to measure other analytes interacting with the magnetic nanoparticles. The integration of magnetic sensors with microfluidic chips reduces the distance between the magnetic nanoparticles on the sensor, lowers the preparation time, and increases the sensor sensitivity [15]. Therefore, this work aims to develop a sensitive method (through magnetic preconcentration of nanoparticles in a microfluidic chip) and cost-effective (though utilization of PEDD technology) for the determination of magnetite in water. To our knowledge, this is the first report on the magnetic preconcentration and photometric determination of magnetite nanoparticles in microfluidic chips.

EXPERIMENTAL

Materials and Apparatus

All reagents and chemicals have analytical purity and were obtained from Merck Company (Darmstadt, Germany). The UV-Vis spectra were recorded using a single beam spectrophotometer WPA model Lightwave II utilizing a quartz cell with a path length of 1 cm. A scale with an accuracy of four decimal places was used to weigh the chemical compounds and a 40 kHz ultrasonic cleaner water

bath (RoHS, Korea) was used to mix and dissolve the chemicals. A 100 W CO₂ infrared laser device (Rotec RT6040, Iran) was used for the construction of microfluidic chips. The solutions were pumped using a peristaltic pump (Ismatec MPC). For the PEDD system, a green LED lamp was used as a light source, and a red LED lamp was used as a detector. A VICTOR88C model digital multimeter with an accuracy of 0.1 mV was used to measure the potential difference between the two ends of the anode and cathode of the red LED. A direct current power supply was used to apply the potential difference between the two ends of the green lamp. A square-shaped NdFeB magnet was used for the preconcentration of the magnetic nanoparticles inside the chip. Heater stirrer and steel clamps were used to thermally connect the chip layers.

The magnetic properties of synthesized magnetic nanoparticles were measured with a vibrating sample magnetometer (VSM, 4 in. Daghigh Meghnatis Kashan Co., Kashan, Iran). The morphological features of the sample were investigated with a Zeiss (Germany) transmission electron microscope (TEM) operating at 100 kV. The magnetization curve of the magnetite nanoparticles recorded with VSM is illustrated in Fig. 1a. As shown in Fig. 1a, the magnetization of the samples would approach the saturation values when the applied magnetic field increases to 10,000 Oe. The saturation magnetization of the magnetite nanoparticles was 67.26 emu g⁻¹. The TEM images (Fig. 1b) showed that spherical magnetic nanoparticles with a narrow size distribution of 9.2 ± 1.8 nm have been successfully synthesized.

Synthesis of Magnetite Nanoparticles

In this research, magnetic iron nanoparticles were synthesized by the co-precipitation method in which 2 grams of FeCl₃·6H₂O (0.0074 mol) and 0.74 grams of FeCl₂·4H₂O (0.0037 mol) were poured into 100 ml of water and stirred magnetically [16,17]. The ratio of [Fe³⁺]/[Fe²⁺] was around 2.0. Then the temperature of the solution was set to 80 °C. Then, an appropriate amount of ammonia was added to the said solution at once to adjust the pH of the solution to about 11. As soon as ammonia was added, the color of the solution turned black, which indicates the synthesis of magnetite nanoparticles. The mixture was stirred under these conditions for 1 hour. Then, the synthesized magnetite nanoparticles were separated from the mixture using a permanent magnet and purified by washing four times consecutively with deionized water and ethanol using magnetic decantation. Finally, the synthesized nanoparticles were placed in an autoclave for 24 hours to dry completely. The total weight of synthesized magnetite nanoparticles was 0.713 g which indicates a synthesis yield of 82.7%.

Chip Fabrication

SolidWorks 2021 software is used to design the microfluidic chip. Several designs were tried to solve the microchannel blockage due to the magnetic capture of magnetite nanoparticles. In all designs, when the entrance for all channels was identical in geometry, all channels were blocked close to the entrance point. However, in the optimum design (Fig. 2) which the entrance for channels is different in

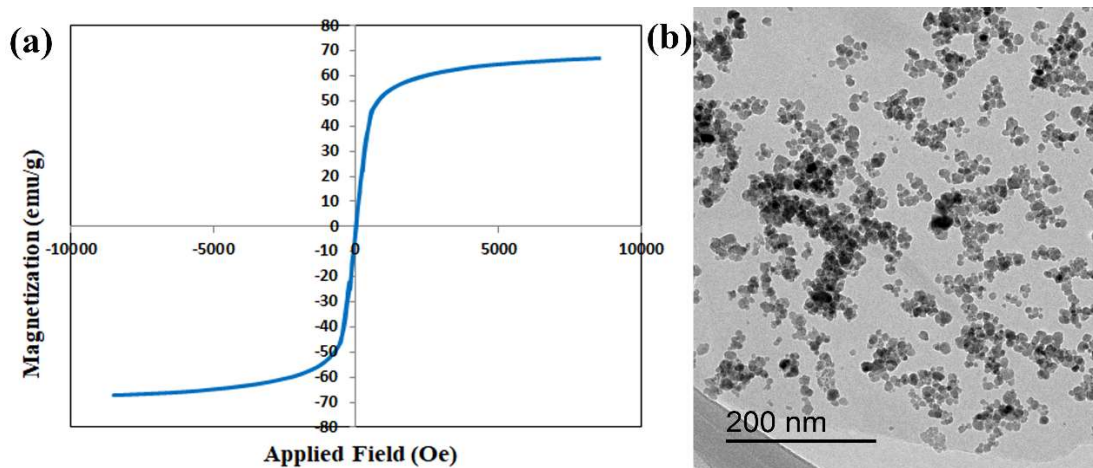


Fig. 1. The VSM curve (a) and TEM image (b) of the synthesized magnetite nanoparticles.

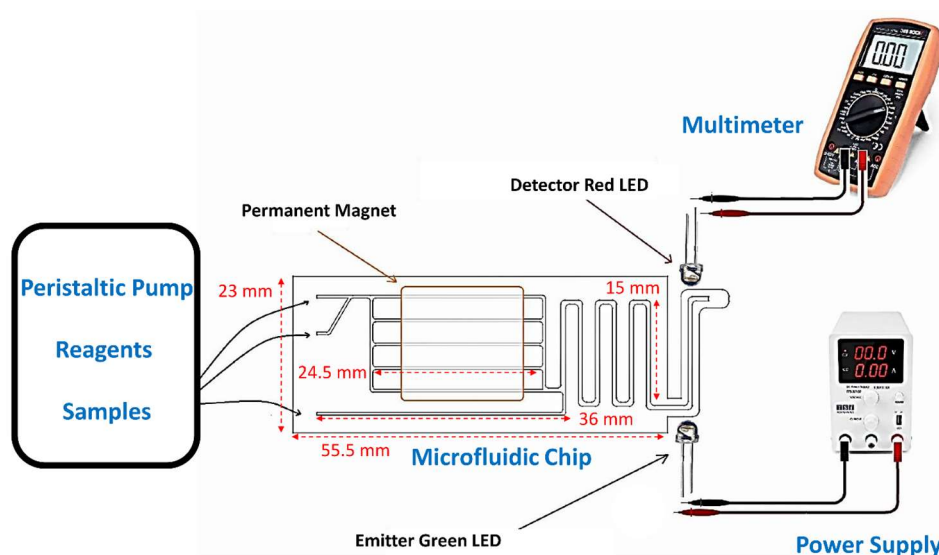


Fig. 2. The developed device and procedure for preconcentration and determination of magnetite nanoparticles.

geometry, when the upper channel is blocked, the solution flows through other channels. Thus, all channels were utilized for the nanoparticle capture. The design had three inputs and one output. The diameter of each inlet channel was considered $200\ \mu\text{m}$ (except for sodium thiocyanate inlet, which was $400\ \mu\text{m}$), and after connecting the channels, the diameter of the channel increased to $600\ \mu\text{m}$. The diameter of the channels is considered so that solutions with higher viscosity than water do not block the channels and the flow created by the peristaltic pump is not reversed. Transparent polymethyl methacrylate (PMMA) sheets with a diameter of $2.7\ \text{mm}$ were used to fabricate the microfluidic chip. The height of the laser head was set to $8\ \text{mm}$ from the surface of the polymer sheet. PMMA sheets were engraved by laser (power: 16% , speed: $150\ \text{mm s}^{-1}$, interval: $2.5\ \mu\text{m}$) and were cut according to the design using a laser machine. Then the microchannels were washed using 1-propanol in an ultrasonic bath and washed with deionized water. Two pieces of cut PMMA sheets, one with microchannels, inlet, and outlet, and the other without channels, were glued together thermally.

Analytical Procedure for Preconcentration and Determination of Magnetite Nanoparticles

First, the sample containing magnetite nanoparticles was introduced into the microchip by pump, and in the straight channels, they are trapped by the magnet inside the chip

(Fig. 2). When the sample inlet tubes are inside the sample, the tube is for entering the sodium thiocyanate solution was in deionized water, and after the sample enters, the sample inlet tubes are placed into deionized water for a washing step to remove interferences. Then, the tube connected to the thiocyanate inlet was placed inside the sodium thiocyanate solution so that the sodium thiocyanate solution passed through the channels. After that, the sample inlet tubes were put into the acid at the same time, which dissolves the nanoparticles and produces positive Fe^{3+} ions, and then a complex is formed in the reaction between the Fe^{3+} ion and the thiocyanate ion (red-colored complex). When the colored complex passes in front of the green LED source lamp, it absorbs the light and reduces the light reaching the detector LED. The reduction of this light causes a reduction in the amount of potential difference between the two ends of the detector LED. All measurements were performed in a dark environment to avoid the interference of ambient light.

The method of signal reading is that a video was taken of the changes in the potential value of the two ends of the detector LED, which is recorded by a multimeter, and then a picture was taken from the video every 0.5 seconds using the VideoPhotos android application, and the displayed numbers of the multimeter were extracted and entered into the Excel program. Then the graph of potential changes was drawn in terms of time. To find the best fitting line from the data, the Trendline tool and the Polynomial part with the value of order

equal to 4 (to create the most adaptation) were used. Then, the area under the peaks was calculated and used as the analytical signal.

RESULTS AND DISCUSSIONS

Method Optimization

Optimizing the concentration of sodium thiocyanate solution. Volumes of 25 ml of magnetite nanoparticles with a concentration of 50 ppm were pumped into the chip with a flow rate of 0.1 ml s^{-1} . Then, the trapped nanoparticles were washed with deionized water. In the next step, simultaneously, 37% hydrochloric acid and sodium thiocyanate solutions with different concentrations were pumped into the chip at a flow rate of 0.1 ml s^{-1} in separate experiments. The voltage applied to the source lamp was set to 2.2 V and the response of the detector lamp was recorded as a function of time. The obtained signal was then processed. In Fig. 3a, the resulting signal is plotted as a function of the

concentration of sodium thiocyanate solution. As it is clear from the results, the signal increases with increasing concentration of sodium thiocyanate solution and then decreases at high concentrations. This reduction of the signal can be interpreted according to the reduction of the light incident on the detector and the noise interference of the system. Therefore, 1.5 M concentration of sodium thiocyanate was selected as the optimal value for the next steps.

Optimizing the type of acid. To optimize the type of acid and its concentration, solutions of magnetite nanoparticles with a concentration of 50 ppm and a volume of 25 ml were pumped inside the chip with a flow rate of 0.1 ml s^{-1} . Then the trapped nanoparticles were washed with deionized water. In the next step, sodium thiocyanate solutions with a concentration of 1.5 M and a combination of different percentages of two acids, hydrochloric acid, and nitric acid with a total concentration of 11.87 M (pure hydrochloric acid solution, pure nitric acid solution, and a

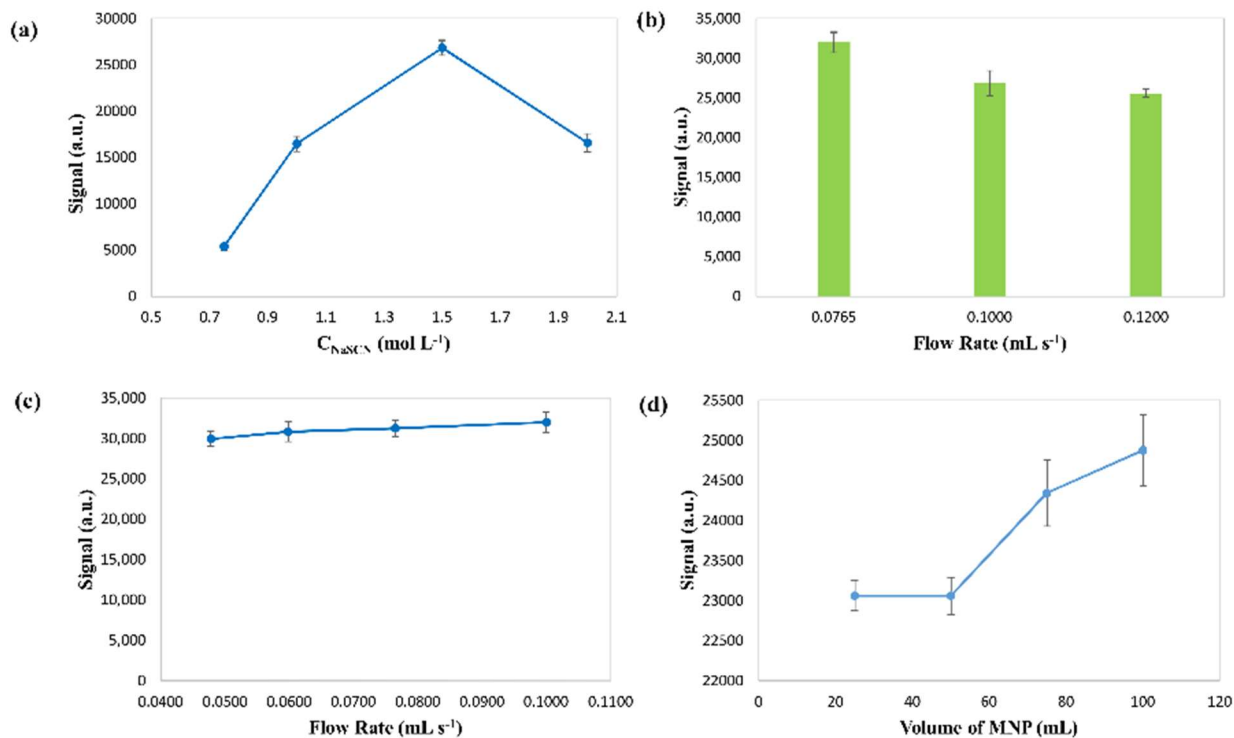


Fig. 3. The effect of sodium thiocyanate concentration (a), flow rate in the nanoparticles dissolution step (b), nanoparticle entrapment flow rate (c), and sample volume (d) on the signal recorded using the developed method (conditions: sample volume for Fig. 3a, 3b, and 3d, 25 ml; nanoparticles concentration, 50 ppm; voltage applied to the source lamp, 2.2 V; nanoparticle entrapment flow rate for Fig. 3a, 0.1 ml s^{-1} ; sodium thiocyanate concentration for Fig. 3b, 3c, and 3d, 1.5 M).

mixture of these two with 3:1 ratio) was pumped into the chip at a flow rate of 0.1 ml s^{-1} in separate experiments. The voltage applied to the source lamp was set to 2.2 V and the response of the detector lamp was recorded as a function of time. The results showed that the presence of nitric acid causes a significant increase in the signal, but in this case, the dissolution time of the nanoparticles is longer, and the production of orange-colored nitrogen dioxide gas inside the system causes signal reading errors. For this reason, 37% hydrochloric acid was used as the acid for subsequent experiments.

Optimizing the effect of flow rate in the nanoparticles dissolution step. To optimize the effect of the flow rate of sodium thiocyanate and hydrochloric acid solutions, first, the solution of magnetite nanoparticles with a concentration of 50 ppm and a volume of 25 ml was pumped into the chip with a flow rate of 0.1 ml s^{-1} . Then, the trapped nanoparticles were washed with deionized water. In the next step, sodium thiocyanate solutions with a concentration of 1.5 M and 37% hydrochloric acid were simultaneously pumped into the chip in separate experiments with different flow rates. The voltage applied to the source lamp was set to 2.2 V and the response of the detector lamp was recorded as a function of time. The results showed that (Fig. 3b), the signal decreases with increasing the flow rate. The reason for this could be the less chance for the dissolution of trapped nanoparticles and the interaction of produced iron ions with thiocyanate. Therefore, according to the results, the flow rate of 0.0765 ml s^{-1} was chosen as optimal. It should be noted that the lower flows were not studied due to the long time of dissolution and measurement.

Optimizing the nanoparticle entrapment flow rate. To optimize the effect of the flow rate of the sample solution containing nanoparticles, first, the solution of iron nanoparticles with a concentration of 50 ppm and a volume of 25 ml was pumped into the chip with different flow rates. Then the trapped nanoparticles were washed with deionized water. In the next step, sodium thiocyanate solutions with a concentration of 1.5 M and 37% hydrochloric acid were simultaneously pumped into the chip in separate experiments with a flow rate of 0.0765 ml s^{-1} . The voltage applied to the source lamp was set to 2.2 V and the response of the detector lamp was recorded as a function of time. The results showed that (Fig. 3c) the flow rate does not show a significant change

in the studied range. The result can be attributed to the effective magnetic trapping of the nanoparticles inside the chip over the studied flow rates. According to the obtained data, the flow rate of 0.0765 ml s^{-1} was chosen because the lower flow rate prolongs the trapping time of nanoparticles and also results in increasing the measurement time.

Effect of sample volume. To investigate the effect of sample volume, different volumes of 1 ppm solution of nanoparticles were pumped into the chip under optimal conditions and the signal was drawn as a function of sample volume (Fig. 3d). The results showed that by increasing the sample volume for a fixed concentration of nanoparticles, the signal increases, but the measurement time also becomes longer. The signal enhancement can be attributed to a higher weight of trapped nanoparticles for higher sample volumes. Therefore, the volume of 75 ml was chosen as optimal.

Method Validation

To evaluate the efficiency of the proposed method, the developed method was evaluated in terms of sensitivity, accuracy, and precision for the determination of magnetite nanoparticles in water samples. Various and specific amounts of nanoparticles were added to 75 ml volumes of urban water samples. The samples were pumped into the microchip in 3 consecutive experiments. Then the trapped nanoparticles were washed with deionized water. In the next step, sodium thiocyanate solutions with a concentration of 1.5 M and 37% hydrochloric acid were simultaneously pumped into the chip in separate experiments with a flow rate of 0.0765 ml s^{-1} . The voltage applied to the source lamp was set to 2.2 V and the response of the detector lamp was recorded as a function of time. Then the obtained signal was converted into concentration using the obtained calibration equation, and the average concentration obtained was used to calculate the percentage of recovery and coefficient of variation. The limit of detection (LOD) and the limit of quantification (LOQ) were calculated according to the IUPAC recommendation ($\text{LOD} = 3s_b/m$, $\text{LOQ} = 10s_b/m$; where s_b is the standard deviation of the blank solution and m is the slope of the calibration equation).

To draw the calibration curve, first, 75 ml of magnetite nanoparticle solution with different concentrations was pumped inside the chip with a flow rate of 0.0765 ml s^{-1} . Then the trapped nanoparticles were washed with deionized water.

In the next step, sodium thiocyanate solutions with a concentration of 1.5 M and 37% hydrochloric acid were simultaneously pumped into the chip in separate experiments with a flow rate of 0.0765 ml s⁻¹. The voltage applied to the source lamp was set to 2.2 V and the response of the detector lamp was recorded as a function of time. The results showed that the resulting signal has a good correlation with the concentration of nanoparticles in the range of 1.0 to 6.0 ppm (Signal (a.u.) = 274.75C_{MNP} + 24066 R² = 0.9841). The values of LOD and LOQ were obtained as 0.3 and 0.9 ppm, respectively. To estimate the precision of the results, 75 ml of the samples with concentrations of 2.5 and 4.5 ppm were pumped into the microchip in three consecutive tests. Then the obtained signals were converted to concentration using the obtained calibration equation and the coefficient of variation (CV) was calculated. The CV for the concentration of 2.5 and 4.5 ppm under optimal conditions was 0.17% and 0.15%, which indicates the high repeatability of the method. To evaluate the accuracy of the obtained results, spiked/recovery experiments were conducted. 75 ml tap water samples were spiked with magnetite nanoparticles at two concentration levels of 2.5 and 4.5 ppm. The samples were pumped into the microchip in three consecutive tests. Then, the obtained signals were converted into concentration using the obtained calibration equation, and the average concentration obtained was calculated as 2.6 and 4.3 ppm, respectively. According to the result, the recovery percentages were 104.0% and 95.6%, respectively, which indicates the appropriate accuracy of the method. It is worth mentioning that non-spiked samples showed no detectable nanoparticles. Compared to previously reported methods, the developed method provides higher sensitivity and spectrophotometry (1-20 ppm_{Fe} for ICP-OES, 2.5-20 ppm_{Fe} for spectrophotometry) methods [3], and the smartphone colorimetric method [4]) and simpler instrumentation of lower analysis cost (compared to solid-phase NMR-relaxometry [2]) by the use microfluidic chip for magnetic preconcentration of magnetic nanoparticles, washing, dissolution, and photometric determination.

CONCLUSIONS

Due to the increasing use of these magnetic nanoparticles, it is important to measure these nanoparticles in different

samples. In this research, for the first time, a microfluidic-based method was developed for the preconcentration and measurement of magnetite magnetic nanoparticles. The basis of work of the designed system is based on the magnetic trapping of nanoparticles inside the microchip, dissolution by acid, and creation of a signal through the formation of an iron-thiocyanate complex. In this research, the coupled light-emitting diode-detector photometry technique was used to read the signal. The validation results of the method showed that the linear range of the method is from 1.0 to 6.0 ppm with proper accuracy and precision, which is satisfactory for measuring trace amounts of magnetite nanoparticles. Limitations and disadvantages of the developed method are the inability to distinguish between various iron-oxide and ferrite nanoparticles since the detection is based on the iron ions, not the nanoparticles directly. This limitation can be resolved by the use of multiple detection approaches. Also, the instability of light intensity of the emitter LED can be resolved by the use of more advanced light sources.

REFERENCES

- [1] Y. Al-Eryani, M. Dadashi, S. Aftabi, H. Sattarifard, G. Ghavami, Z.W. Oldham, A. Ghoorchian, S. Ghavami, 4 - Toxicity, therapeutic applicability, and safe handling of magnetic nanomaterials, in: M. Ahmadi, A. Afkhami, T. Madrakian (Eds.), *Magnetic Nanomaterials in Analytical Chemistry*, Elsevier2021, pp. 61-83.
- [2] A.S. Minin, M.A. Uymin, A.Y. Yermakov, I.V. Byzov, A.A. Mysik, M.B. Rayev, P.V. Khrantsov, S.V. Zhakov, A.V. Volegov, I.V. Zubarev, Application of NMR for quantification of magnetic nanoparticles and development of paper-based assay, *J. Phys. Conf. Ser.* 1389 (2019) 012069.
- [3] R. Costo, D. Heinke, C. Grüttner, F. Westphal, M.P. Morales, S. Veintemillas-Verdaguer, N. Gehrke, Improving the reliability of the iron concentration quantification for iron oxide nanoparticle suspensions: a two-institutions study, *Anal. Bioanal. Chem.* 411 (2019) 1895.
- [4] Y. Fernández-Afonso, G. Salas, I. Fernández-Barahona, F. Herranz, C. Grüttner, J. Martínez de la Fuente, M. del Puerto Morales, L. Gutiérrez, Smartphone-Based Colorimetric Method to Quantify Iron Concentration and

- to Determine the Nanoparticle Size from Suspensions of Magnetic Nanoparticles, *Part. Part. Syst. Charact.* 37 (2020) 2000032.
- [5] N. Holonyak Jr, S.F. Bevacqua, Coherent (visible) light emission from Ga (As_{1-x}P_x) junctions, *Appl. Phys. Lett.* 1 (1962) 82.
- [6] M. L.C. Passos, M.L. M.F.S. Saraiva, Detection in UV-visible spectrophotometry: Detectors, detection systems, and detection strategies, *Measurement* 135 (2019) 896.
- [7] S. Thomas, M. Ahmadi, T.A. Nguyen, A. Afkhami, T. Madrakian, *Micro- and Nanotechnology Enabled Applications for Portable Miniaturized Analytical Systems*, Paperback ISBN: 9780128237274, eBook ISBN: 9780128237281, 2021.
- [8] N. Bastan, M. Ahmadi, T. Madrakian, A. Afkhami, S. Khalili, M. Majidi, M. Moradi, A paired emitter–detector diode-based photometer for the determination of sodium hypochlorite adulteration in milk, *Sci. Rep.* 13 (2023) 6217.
- [9] F. Ghobadi Seresht, M. Ahmadi, S. Khalili, M. Majidi, Determination of 2, 4, 6-Trinitrotoluene in Soil Samples Using a Paired Emitter-Detector Diode-Based Photometer, *Anal. Bioanal. Chem. Res.* 10 (2023) 149.
- [10] M. O’Toole, D. Diamond, Absorbance Based Light Emitting Diode Optical Sensors and Sensing Devices, *Sensors* 8 (2008) 2453.
- [11] Z. Amouzegar, N. Rezvani Jalal, M. Kamalabadi, M. Abbasi Tarighat, A. Afkhami, T. Madrakian, S. Thomas, T.A. Nguyen, M. Ahmadi, Chapter 2 - Spectrometric miniaturized instruments, in: S. Thomas, M. Ahmadi, T.A. Nguyen, A. Afkhami, T. Madrakian (Eds.), *Micro- and Nanotechnology Enabled Applications for Portable Miniaturized Analytical Systems*, Elsevier 2022, pp. 17-40.
- [12] L. Barron, M. O’Toole, D. Diamond, P.N. Nesterenko, B. Paull, Separation of transition metals on a poly-iminodiacetic acid grafted polymeric resin column with post-column reaction detection utilising a paired emitter-detector diode system, *J. Chromatogr. A* 1213 (2008) 31.
- [13] M. O’Toole, L. Barron, R. Shepherd, B. Paull, P. Nesterenko, D. Diamond, Paired emitter-detector diode detection with dual wavelength monitoring for enhanced sensitivity to transition metals in ion chromatography with post-column reaction, *Analyst* 134 (2009) 124.
- [14] D. Murzin, D.J. Mapps, K. Levada, V. Belyaev, A. Omelyanchik, L. Panina, V. Rodionova, Ultrasensitive Magnetic Field Sensors for Biomedical Applications, *Sensors* 20 (2020).
- [15] R. Abedini-Nassab, M. Pouryosef Miandoab, M. Şaşmaz, Microfluidic Synthesis, Control, and Sensing of Magnetic Nanoparticles: A Review, *Micromachines* 12 (2021).
- [16] T. Madrakian, R. Haryani, M. Ahmadi, A. Afkhami, A sensitive electrochemical sensor for rapid and selective determination of venlafaxine in biological fluids using carbon paste electrode modified with molecularly imprinted polymer-coated magnetite nanoparticles, *J. Iran. Chem. Soc.* 13 (2016) 243.
- [17] T. Madrakian, B. Zadpour, M. Ahmadi, A. Afkhami, Selective extraction and sensitive determination of mercury(II) ions by flame atomic absorption spectrometry after preconcentration on an ion-imprinted polymer-coated maghemite nanoparticles, *J. Iran. Chem. Soc.* 12 (2015) 1235.